View metadata, citation and similar papers at core.ac.uk

brought to you by CORE

provided by HKU Scholars Hub

The HKU Scholars Hub The University of Hong Kong 香港大學學術庫

Title	Single-photon transport in a one-dimensional waveguide coupling to a hybrid atom-optomechanical system
Author(s)	Jia, W; Wang, Z
Citation	Physical Review A (Atomic, Molecular and Optical Physics), 2013, v. 88 n. 6, p. article no. 063821
Issued Date	2013
URL	http://hdl.handle.net/10722/195689
Rights	Creative Commons: Attribution 3.0 Hong Kong License

Single-photon transport in a one-dimensional waveguide coupling to a hybrid atom-optomechanical system

W. Z. Jia[1,2] and Z. D. Wang[1,*]

[1]*Department of Physics and Center of Theoretical and Computational Physics, The University of Hong Kong, Pokfulam Road, Hong Kong, China*

[2]*Quantum Optoelectronics Laboratory, School of Physical Science and Technology, Southwest Jiaotong University, Chengdu 610031, China*

(Received 8 August 2013; published 10 December 2013)

We explore theoretically the single-photon transport in a single-mode waveguide that is coupled to a hybrid atom-optomechanical system in a strong optomechanical coupling regime. Using a full quantum real-space approach, transmission and reflection coefficients of the propagating single-photon in the waveguide are obtained. The influences of atom-cavity detuning and the dissipation of atom on the transport are also studied. Intriguingly, the obtained spectral features can reveal the strong light-matter interaction in this hybrid system.

DOI: 10.1103/PhysRevA.88.063821 PACS number(s): 42.50.Pq, 42.50.Wk, 42.79.Gn, 07.10.Cm

I. INTRODUCTION

Recently, research of controllable single-photon transport in low-dimensional systems has attracted growing interest because of its significant importance in quantum control, including quantum information processing. Usually this kind of manipulation is achieved by strongly coupling a propagating single photon in the waveguide to a local quantum system [1–3]. A desired single-photon control process results from an interference between the directly transmitted photon and the photon re-emitted by the emitter. Specifically, such a waveguide-emitter system can be realized by a photonic nanowire with an embedded quantum dot [4], surface plasmons coupled to a single two-level emitter [5], a superconducting transmission line coupled to a superconducting artificial atom [6], or a single-mode waveguide coupled to a cavity interacting with a two-level atom [7–10].

As is known, a new type of optomechanical cavity was also developed to couple photons and phonons via radiation pressure. Significant research interest in this frontier of optomechanics is motivated by its potential applications in ultrasensitive measurements, quantum information processing, and implementation of novel quantum phenomena at macroscopic scales [11–13]. Typically, if an optomechanical system works in the single-photon strong-coupling regime, the radiation pressure from a single photon can even produce observable effects. Specifically, a single-photon coupling strength larger than the cavity decay rate may define the regime where coherent optomechanical interaction takes place; and a coupling strength larger than the frequency of mechanical resonator means that multiphonon processes take place in the interactions. Although the single-photon strong-coupling regime has not yet been reached except for analogous cold atom experiments [14–16]. But recent experiments based on superconducting devices [17], optomechanical crystal cavity [18,19], and spoke-anchored toroidal optical microcavity [20] have already shown huge progress. This progress also inspired a series of theoretical investigations, including photon blockade [21–23] and photon-induced tunneling [24], single-photon cooling [25], optomechanically induced transparency in the single-photon strong-coupling regime [26], and optomechanical instability [27]. Typically, in most quantum optomechanical devices, the cavity is side or direct coupled to a waveguide [13]. Thus in the single-photon regime, optomechanical systems, rather than traditional quantum emitters, may enable us to control the propagating single-photon in the waveguide. Moreover, the single-photon transmission spectra can be used to probe and characterize the strong-coupling regime [28,29]. We also note that, although the regime of single-photon strong optomechanical coupling is still difficult for experimental realization, some recent works have studied the nonlinear effects in the relatively weak optomechanical coupling regime [30–32].

In this paper, we explore theoretically the single-photon transport in a single-mode waveguide coupled to a hybrid atom-optomechanical system in the single-photon strong-coupling regime. Recently, a related scheme was proposed to achieve the strong coupling between the center-of-mass motion of a single trapped atom and the motion of a membrane [33]. Here we wish to indicate that the hybrid atom-optomechanical system considered in this work is realized by coupling an optomechanical cavity to the atomic internal degrees of freedom (the center-of-mass motion of atom is neglected). Notably, a weak continuous-wave laser scattering problem in this hybrid atom-optomechanical system was perturbatively treated in a recent study by assuming the weak optomechanical coupling [34]. Here, we employ a full quantum-mechanical approach [1,2,29] to study the transmission and reflection properties of the propagating photon in the waveguide. In our treatment, we focus on the strong optomechanical coupling regime, where multiple phonons are involved in the scattering. Moreover, the transport of a nonmonochromatic incident photon in the form of a wave packet is studied. Our results also show that the single-photon transmission and reflection spectra can be used to probe and characterize the strong optomechanical and atom-light interactions. Finally, we solve the response of this system to a single photon instead of a continuous drive, for controllable single-photon transport is of central importance in the future quantum devices [1,2].

The paper is organized as follows. In Sec. II, we introduce our model for describing the single-photon transport. Then, in

*zwang@hku.hk

 ©2013 American Physical Society

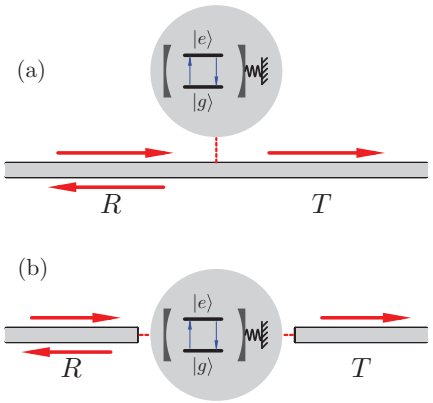

FIG. 1. (Color online) Schematic plot of a coupling system considered here. An optomechanical cavity interacting with a two-level atom is coupled to a single-mode waveguide, in which single photons propagate along the arrow direction. (a) Side-coupled cases. (b) Direct coupled cases.

Sec. III, we look into the single-photon transport properties in detail. The influences of detuning and dissipation are also addressed. Finally, further discussions and conclusions are given in Sec. IV.

II. HAMILTONIAN AND THE SOLUTIONS

We consider a hybrid atom-optomechanical system (i.e., a single two-level atom coupled to an optomechanical cavity) to be coupled to a single-mode waveguide. With well-developed techniques for confining a single atom in a usual optical cavity [35], it seems achievable in the near future to couple atoms with optomechanical cavities. Usually, the atom-optomechanical system can either side-coupled or directly coupled to a waveguide, which is schematically illustrated in Figs. 1(a) and 1(b). In this paper, we focus on the single-photon transport problem of the side-coupling case, for one can straightforwardly map the reflection amplitude of the side-coupled case into the transmission amplitude of the direct-coupled cases [2]. We assume a linear dispersion relation of the waveguide optical mode. In addition, we take narrow bandwidth approximation and decompose the optical field propagating in the waveguide into two distinct contributions with right- and left-moving modes. Finally, the Markov approximation and rotating-wave approximation are assumed. Consequently, the effective Hamiltonian of this system may be written as ($\hbar = 1$)

$$\begin{aligned}\hat{H} =& \int dx a_R^\dagger(x)\left(-iv_g\frac{\partial}{\partial x}\right)a_R(x)\\ &+\int dx a_L^\dagger(x)\left(iv_g\frac{\partial}{\partial x}\right)a_L(x)\\ &+\frac{\omega_a}{2}\sigma_z - i\gamma_a|e\rangle_a\langle e|_a+\omega_c c^\dagger c\\ &+\Omega b^\dagger b - g_0 c^\dagger c(b+b^\dagger)+\lambda(c\sigma^+ + c^\dagger\sigma^-)\\ &+V\int dx\delta(x)(a_R^\dagger(x)c + a_R(x)c^\dagger + a_L^\dagger(x)c + a_L(x)c^\dagger).\end{aligned} \tag{1}$$

The first and second lines denote the waveguide optical mode, where v_g is the group velocity of the photons and $a_R^\dagger(x)$ ($a_L^\dagger(x)$) is a bosonic operator creating a right-going (left-going) photon at x. The third and fourth lines describe the isolated atom-optomechanical system, where $c^\dagger$ ($b^\dagger$) is the photon (phonon) creation operator and $\sigma^+(\sigma^-)$ is the atomic raising (lowering) operator generating transition between ground state and exited state: $\sigma^+|g\rangle_a = |e\rangle_a$, $\sigma^-|e\rangle_a = |g\rangle_a$ [36]. ω_a is the atomic transition frequency, ω_c is the cavity resonance frequency, Ω is the mechanical frequency, g_0 is the single-photon coupling strength of the radiation pressure between the cavity and the mirror, and λ is the coupling strength between the cavity and the atom. The fifth line represents the coupling between the waveguide and the atom-optomechanical system, where V is the coupling strength between the cavity and the waveguide. The according cavity-waveguide's decay rate can be defined as $\Gamma = V^2/v_g$. Note that in our treatment, an imaginary term is included to model the spontaneous emission of the atom at the rate γ_a, due to coupling to the reservoir [2]. In addition, we assume that the majority of the decayed light from the cavity is guided into waveguide modes, i.e., "strong coupling" exists between the cavity and the waveguide [37]. Thus the decay rate κ of the cavity into channels other than the one-dimensional continuum is negligible. We also assume that the decay rate γ_M of the mirror motion is much smaller than the cavity-waveguide's decay rate. As a result, $\Gamma \gg \kappa, \gamma_M$, the optomechanical decoherence processes can safely be ignored, and the main dissipative processes leading to loss of photons are originated from the decay of atom γ_a. Experimentally, in both typical cavity QED and solid-state circuit QED systems, the ratio between the atom (artificial atom) decay rate and the cavity decay rate is about $\gamma_a/\Gamma \sim 0.1$ [38].

For an input one-photon Fock state, the stationary state of the system satisfies the eigenequation

$$H|\epsilon\rangle = \epsilon|\epsilon\rangle. \tag{2}$$

We assume that, initially, the mirror is in state $|n_0\rangle_b$, the atom is in the ground state, the cavity is empty, and a single-photon comes from the left with energy $v_g k$ with k as the wave vector of the photon. In this case, the total energy of the coupled system is $\epsilon = -\omega_a/2 + v_g k + n_0\Omega$. In the single-photon subspace, $|\epsilon\rangle$ can be expanded as

$$\begin{aligned}|\epsilon\rangle =& \sum_n \int dx\varphi_R(x,n)a_R^\dagger(x)|\varnothing\rangle|n\rangle_b\\ &+\sum_n\int dx\varphi_L(x,n)a_L^\dagger(x)|\varnothing\rangle|n\rangle_b\\ &+\sum_n e_n c^\dagger|\varnothing\rangle|\tilde{n}\rangle_b + \sum_n f_n\sigma^+|\varnothing\rangle|n\rangle_b,\end{aligned} \tag{3}$$

where $|\varnothing\rangle = |0\rangle_k|0\rangle_c|g\rangle_a$ is the vacuum state, with zero photon in both the waveguide and the cavity and with the atom in the ground state. $|n\rangle_b$ represents the number state of the mechanical mode. $\varphi_{R,L}(x,n)$ is the single-photon wave function in the R/L mode. e_n and f_n are excitation amplitudes of the cavity and the atom, respectively. $|\tilde{n}\rangle_b = \exp[\frac{g_0}{\Omega}(b^\dagger - b)]|n\rangle_b$ is the single-photon displaced number state of the mechanical oscillator satisfying the eigenequation

$$\begin{aligned}&[\omega_c c^\dagger c + \Omega b^\dagger b - g_0 c^\dagger c(b+b^\dagger)]|1\rangle_c|\tilde{n}\rangle_b\\ &\quad=(\omega_c + n\Omega - \delta)|1\rangle_c|\tilde{n}\rangle_b,\end{aligned} \tag{4}$$

where $\delta = g_0^2/\Omega$ is the photon-state frequency shift caused by a single-photon radiation pressure.

By substituting Eq. (3) into Eq. (2), we obtain the following equations of motion:

$$-iv_g\frac{\partial\varphi_R(x,n)}{\partial x}+\delta(x)V\sum_m e_m U_{nm} = \left(\epsilon+\frac{\omega_a}{2}-n\Omega\right)\varphi_R(x,n), \tag{5a}$$

$$iv_g\frac{\partial\varphi_L(x,n)}{\partial x}+\delta(x)V\sum_m e_m U_{nm} = \left(\epsilon+\frac{\omega_a}{2}-n\Omega\right)\varphi_L(x,n), \tag{5b}$$

$$V\int dx\delta(x)[\varphi_R(x,n)+\varphi_L(x,n)]+\lambda f_n = \sum_m\left(\epsilon+\frac{\omega_a}{2}-\omega_c-m\Omega+\delta\right)e_m U_{nm}, \tag{5c}$$

$$\lambda\sum_m e_m U_{nm} = \left(\epsilon-\frac{\omega_a}{2}-n\Omega+i\gamma_a\right)f_n, \tag{5d}$$

with $U_{nm}=\langle n\mid\tilde{m}\rangle_b$.

Assuming that the mirror is initially prepared in state $|n_0\rangle_b$ and a single-photon comes from the left with energy $v_g k$, $\varphi_R(x,n)$ and $\varphi_L(x,n)$ should take the form

$$\varphi_R(x,n)=\theta(-x)\delta_{nn_0}e^{i\left(k+(n_0-n)\frac{\Omega}{v_g}\right)x}+\theta(x)t_n e^{i\left(k+(n_0-n)\frac{\Omega}{v_g}\right)x}, \tag{6a}$$

$$\varphi_L(x,n)=\theta(-x)r_n e^{-i\left(k+(n_0-n)\frac{\Omega}{v_g}\right)x}, \tag{6b}$$

where t_n and r_n are the transmission and reflection amplitude, respectively. Substituting Eqs. (6a) and (6b) into Eqs. (5a)–(5d), the equations for t_n, r_n, e_n, and f_n are given by

$$-iv_g(-\delta_{nn_0}+t_n)+V\sum_m e_m U_{nm}=0, \tag{7a}$$

$$-iv_g r_n+V\sum_m e_m U_{nm}=0, \tag{7b}$$

$$\frac{1}{2}V[\delta_{nn_0}+t_n+r_n]+\lambda f_n = \sum_m(\Delta_c+(n_0-m)\Omega+\delta)e_m U_{nm}, \tag{7c}$$

$$\lambda\sum_m e_m U_{nm}=(\Delta_c-\Delta_{ac}+(n_0-n)\Omega+i\gamma_a)f_n, \tag{7d}$$

with $\Delta_c=v_g k-\omega_c$, $\Delta_{ac}=\omega_a-\omega_c$. If $\lambda\ll\Gamma,\gamma_a$, we can have the series solutions of r_n and t_n,

$$r_n=-i\Gamma\left(\sum_{n'}\frac{U_{nn'}U^*_{n_0n'}}{\tilde{\Delta}_c(n')}+\sum_{n'mn''}\frac{\lambda^2U_{nn'}U^*_{mn'}U_{mn''}U^*_{n_0n''}}{\tilde{\Delta}_c(n')\tilde{\Delta}_a(m)\tilde{\Delta}_c(n'')}+\sum_{n'mn''m'n'''}\frac{\lambda^4U_{nn'}U^*_{mn'}U_{mn''}U^*_{m'n''}U_{m'n'''}U^*_{n_0n'''}}{\tilde{\Delta}_c(n')\tilde{\Delta}_a(m)\tilde{\Delta}_c(n'')\tilde{\Delta}_a(m')\tilde{\Delta}_c(n''')}+\cdots\right), \tag{8a}$$

$$t_n=\delta_{nn_0}+r_n \tag{8b}$$

with

$$\tilde{\Delta}_c(m)=\Delta_c+(n_0-m)\Omega+\delta+i\Gamma,$$
$$\tilde{\Delta}_a(n)=\Delta_c-\Delta_{ac}+(n_0-n)\Omega+i\gamma_a.$$

The first term in Eq. (8a) represents a single photon directly scattered by the optomechanical cavity without interacting with the atom in it. The following terms correspond to the processes in which the single photon is re-emitted by the cavity after interacting with the atom (i.e., single-photon exchange processes between the cavity and the atom). Thus the reflection amplitude r_n is the quantum interference of all these processes. Equation (8b) shows that the transmission wave is the superposition of the propagating wave in the waveguide without entering the cavity and the re-emitted wave after interaction with the system.

For an arbitrary λ, Eqs. (7a)–(7d) can be solved numerically by choosing the upper limit of n large enough, namely $n_{\max}\gg n_0$, and solving the attained $4(n_{\max}+1)$ equations. Note that r_n (t_n) represents the amplitude of reflecting (transmitting) a single-photon with frequency $v_g k-(n-n_0)\Omega$. Thus the total single-photon transmission and reflection coefficients should be given by

$$T=\sum_n|t_n|^2,\quad R=\sum_n|r_n|^2. \tag{9}$$

More generally, the mechanical resonator can be initially in a pure state (e.g., coherent state) $\sum_{n_0}C_{n_0}|n_0\rangle_b$ or a mixed state (e.g., thermal state) $\sum_{n_0}P_{n_0}|n_0\rangle_b\langle n_0|_b$. The according single-photon transmission and reflection coefficients are

$$T=\sum_n\left|\sum_{n_0}C_{n_0}t_{n_0,n}\right|^2,\quad R=\sum_n\left|\sum_{n_0}C_{n_0}r_{n_0,n}\right|^2 \tag{10}$$

for a pure state and

$$T=\sum_n\sum_{n_0}P_{n_0}|t_{n_0,n}|^2,\quad R=\sum_n\sum_{n_0}P_{n_0}|r_{n_0,n}|^2 \tag{11}$$

for a mixed state, respectively.

III. SINGLE-PHOTON SCATTERING SPECTRA

A. Single-photon transmission (reflection) coefficient: Atom cavity in tune and nondissipative case

We first investigate the single-photon transmission and reflection spectra of an optomechanical cavity containing no atom. Only the sideband-resolved regime $\Gamma\ll\Omega$ is considered in this work. We plot the transmission and reflection coefficient as the functions of the photon-cavity detuning Δ_c for various values of g_0 when the mirror is initially prepared in the ground state $|0\rangle_b$, as shown in Fig. 2. When $g_0=0$, the coherently interference of the leaked waves out of the cavity and the propagating modes in the one-dimensional continuum result in a complete suppression of the transmission for a resonantly incident photon with $\Delta_c=0$. When entering the regime with $g_0\sim\Omega$, where multiphonon processes can take place, the transmission dips (reflection peaks) appear at $\Delta_c=-\delta+n\Omega$ ($n=0,1,2\cdots$), exhibiting a global red shift δ and obvious multisidebands. This means that an incident single-photon with frequency $\omega_c-\delta+n\Omega$ can be strongly reflected by the

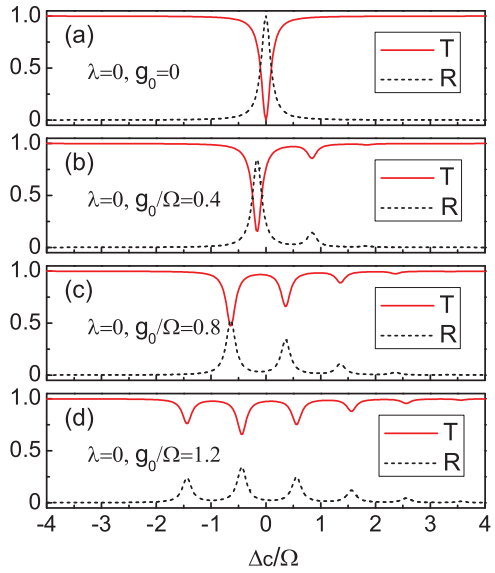

FIG. 2. (Color online) Single-photon transmission (reflection) spectra of a standard optomechanical cavity (i.e., the cavity-atom coupling strength $\lambda = 0$) for various g_0. The cavity-waveguide decay rate $\Gamma = 0.1\Omega$ is chosen for plotting the spectra.

optomechanical system because of the strong optomechanical coupling.

To investigate the single-photon transmission and reflection property of the hybrid atom-optomechanical system, we first give the eigenenergies and eigenstates of an isolate atom-optomechanical system. The Hamiltonian of an isolate atom-optomechanical system can be written as

$$\hat{H}_{AO} = \hat{H}_0 + \hat{H}_I \tag{12}$$

with

$$\hat{H}_0 = \frac{\omega_a}{2}\sigma_z + \omega_c c^\dagger c + \Omega b^\dagger b - g_0 c^\dagger c(b + b^\dagger), \tag{13a}$$

$$\hat{H}_I = \lambda(c\sigma^+ + c^\dagger\sigma^-). \tag{13b}$$

In the single-photon subspace, the eigenstates of $\hat{H}_0$ are $|0\rangle_c|e\rangle_a|n\rangle_b$ with the eigenenergy $\epsilon_{\uparrow n} = \omega_a/2 + n\Omega$ and $|1\rangle_c|g\rangle_a|\tilde{n}\rangle_b$ with the eigenenergy $\epsilon_{\downarrow n} = -\omega_a/2 + \omega_c + n\Omega - \delta$. In this subspace, exact diagonalization of the Hamiltonian $\hat{H}_{AO}$ yields the eigenstates

$$|\psi_n^{(+)}\rangle = \sin\theta|1\rangle_c|g\rangle_a|\tilde{n}\rangle_b + \cos\theta|0\rangle_c|e\rangle_a|n\rangle_b, \tag{14a}$$

$$|\psi_n^{(-)}\rangle = -\cos\theta|1\rangle_c|g\rangle_a|\tilde{n}\rangle_b + \sin\theta|0\rangle_c|e\rangle_a|n\rangle_b, \tag{14b}$$

with the corresponding eigenenergies

$$E_n^{(+)} = \frac{\omega_c}{2} + n\Omega - \frac{\delta}{2} + \frac{1}{2}\sqrt{(\Delta_{ac}+\delta)^2 + 4\lambda^2}, \tag{15a}$$

$$E_n^{(-)} = \frac{\omega_c}{2} + n\Omega - \frac{\delta}{2} - \frac{1}{2}\sqrt{(\Delta_{ac}+\delta)^2 + 4\lambda^2}, \tag{15b}$$

where

$$\theta = \frac{1}{2}\tan^{-1}\frac{2\lambda}{\Delta_{ac}+\delta}.$$

We now consider the case that the two-level atom is in resonance with the cavity, i.e., $\Delta_{ac} = 0$. Here we are especially interested in the following two-parameter regimes: (a) $\lambda \gg \Omega \gg \Gamma$ and $\lambda \gg \delta$; (b) $\lambda < \Gamma$, for the single-photon transmission (reflection) spectrum will show Rabi-splitting like structure in the case (a) and EIT-like one in the case (b), respectively. When the atom-cavity coupling strength satisfies $\lambda \gg \Omega \gg \Gamma$ and $\lambda \gg \delta$, the eigenstates of the atom-optomechanical system take the form

$$|\psi_n^{(+)}t\rangle \sim \frac{1}{\sqrt{2}}(|1\rangle_c|g\rangle_a|\tilde{n}\rangle_b + |0\rangle_c|e\rangle_a|n\rangle_b), \tag{16a}$$

$$|\psi_n^{(-)}\rangle \sim \frac{1}{\sqrt{2}}(|1\rangle_c|g\rangle_a|\tilde{n}\rangle_b - |0\rangle_c|e\rangle_a|n\rangle_b), \tag{16b}$$

with the corresponding eigenenergies

$$E_n^{(+)} \approx \frac{\omega_c}{2} + n\Omega - \frac{\delta}{2} + \lambda, \tag{17a}$$

$$E_n^{(-)} \approx \frac{\omega_c}{2} + n\Omega - \frac{\delta}{2} - \lambda. \tag{17b}$$

The energy-level structure in this case is plotted in Fig. 3(a). When $\lambda < \Gamma$, the eigenstates of the atom-optomechanical system take the form

$$|\psi_n^{(+)}\rangle \sim |0\rangle_c|e\rangle_a|n\rangle_b + \frac{\lambda}{\delta}|1\rangle_c|g\rangle_a|\tilde{n}\rangle_b, \tag{18a}$$

$$|\psi_n^{(-)}\rangle \sim |1\rangle_c|g\rangle_a|\tilde{n}\rangle_b - \frac{\lambda}{\delta}|0\rangle_c|e\rangle_a|n\rangle_b, \tag{18b}$$

with the eigenenergies

$$E_n^{(+)} \approx \frac{\omega_c}{2} + n\Omega + \frac{\lambda^2}{\delta}, \tag{19a}$$

$$E_n^{(-)} \approx \frac{\omega_c}{2} + n\Omega - \delta - \frac{\lambda^2}{\delta}. \tag{19b}$$

The energy-level structure of this case is depicted in Fig. 3(b).

Figures 4 and 5 give the single-photon transmission (reflection) spectra of the two cases. When the atom-cavity coupling strength $\lambda \gg \Omega \gg \Gamma$ and the optmechanical coupling strength $g_0 = 0$, the transmission(reflection) spectrum shows vacuum Rabi splitting [2,7] with the splitting width 2λ, as shown in Fig. 4(a). Figures 4(b)–4(d) show how the moving mirror modifies the vacuum Rabi spectrum in the strong-coupling regime with multiphonon processes taking place. When the coupling strength g_0 increases to be comparable to the mechanical frequency Ω, the spectra will undergo a red shift $\delta/2$. Additionally, on the right side of each main peak, more sidebands will appear with interval Ω, corresponding to the energy levels described in Eqs. (17a) and (17b).

If $\lambda < \Gamma$, we can get a spectrum that is analogous to that for electromagnetically induced transparency (EIT) phenomena [2,39]. Typically, when $g_0 = 0$, the spectrum exhibits a standard EIT one with a very narrow transmission window, as shown in Fig. 5(a). When entering the regime $g_0 \sim \Omega$, more EIT structures appear in the sideband regime [Figs. 5(b)–5(d)]. The transmission maxima are located at $\Delta_c = n\Omega$ ($n = 0,1,2\cdots$). Typically, when $g_0 = \sqrt{m}\Omega$ ($m = 1,2,\cdots$), i.e., $\delta = m\Omega$, we have $\epsilon_{\uparrow n} = \epsilon_{\downarrow n+m} = \omega_c/2 + n\Omega$. Namely, the eigenstates $|0\rangle_c|e\rangle_a|n\rangle_b$ and $|1\rangle_c|g\rangle_a|n \mp m\rangle_b$ of $\hat{H}_0$ are degenerate. This degeneracy is perturbed by the relatively weak atom-cavity interaction H_I, resulting in a pair of near-degenerate states $|\psi_n^{(+)}\rangle$ and $|\psi_{n+m}^{(-)}\rangle$ with eigenenergies $\omega_c/2 + n\Omega \pm \lambda^2/\delta$, as shown in Fig. 3(b). Thus,

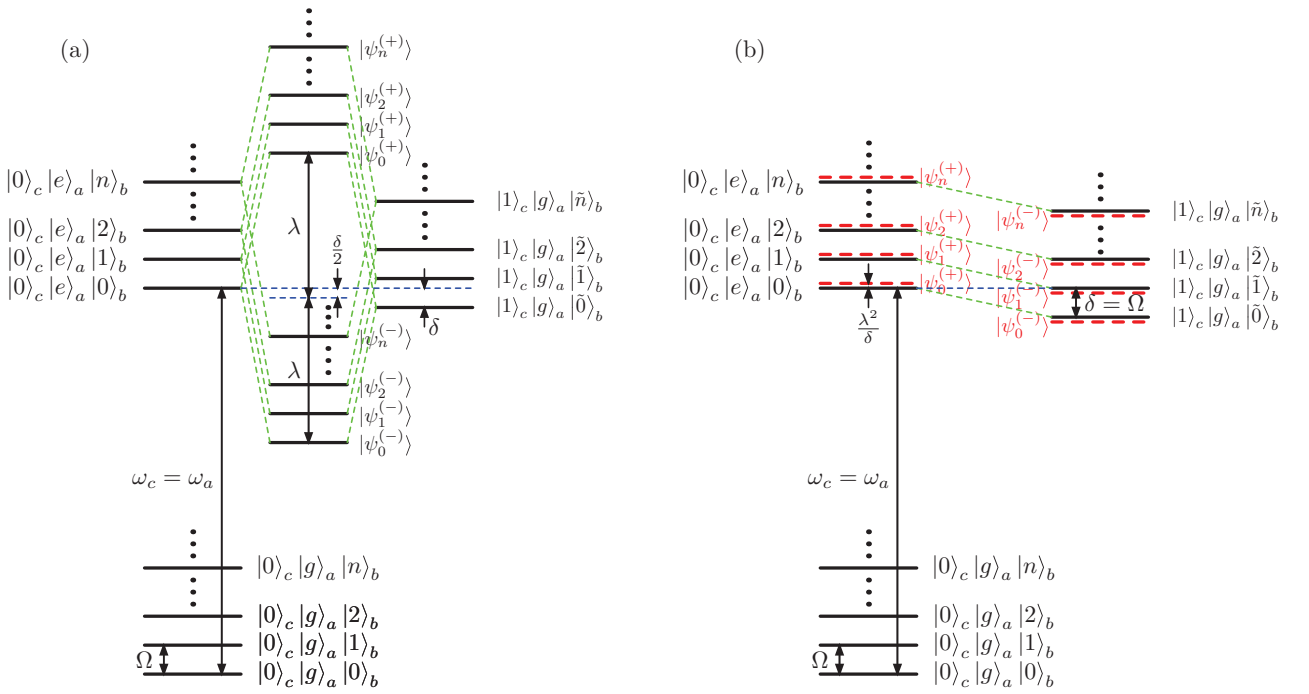

FIG. 3. (Color online) The energy-level structure of a hybrid atom-optomechanical cavity (limited to the zero- and one-photon subspaces) in the single-photon strong-coupling regime, where the two-level atom is in resonance with the cavity (i.e., $\Delta_{ac} = 0$). The atom-cavity coupling strength satisfies $\lambda \gg \Omega \gg \Gamma$ and $\lambda \gg \delta$ for (a) and $\lambda < \Gamma$ with $g_0 = \Omega$ (i.e., $\delta = \Omega$) for (b).

when a single-photon with detuning $\Delta_c = n\Omega$ ($n = 0,1,2\cdots$) is injected, destructive quantum interference occurs between the two possible transition channels $|0\rangle_c|g\rangle_a|0\rangle_b \rightarrow |\psi_n^{(+)}\rangle$ and $|0\rangle_c|g\rangle_a|0\rangle_b \rightarrow |\psi_{n+m}^{(-)}\rangle$, resulting in a complete transmission of the single photon. This generates an EIT-like structure at $\Delta_c = n\Omega$ in the transmission (reflection) spectrum, as seen in Figs. 5(c) and 5(d). This EIT-like phenomenon is very similar to cavity-induced transparency [40] and can be explained in terms of interference effect used in Ref. [34]. Specifically, in our case, when $\Delta_c = n\Omega$ ($n = 0,1,2\cdots$), the states $|1\rangle_c|g\rangle_a|n \mp m\rangle_b$ cannot be populated because of destructive quantum interference in the excitation paths, resulting in direct transmission of the single photon without absorption. The transmission dips (reflection peaks) located at

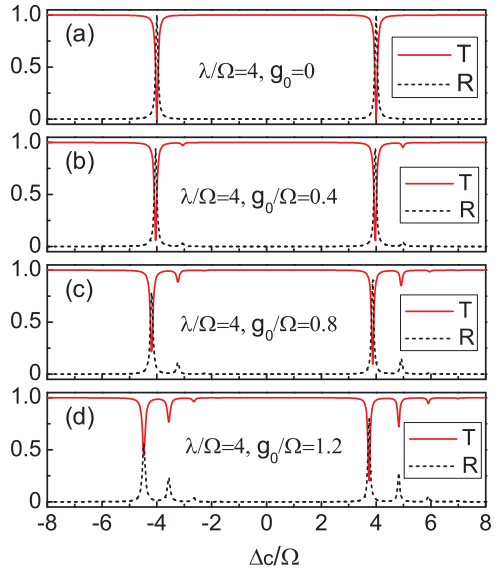

FIG. 4. (Color online) Single-photon transmission (reflection) spectra of the atom-optomechanical system for $\lambda \gg \Gamma$. The parameters are $\lambda = 4\Omega$, $\Delta_{ac} = 0$, $\gamma_a = 0$, and $\Gamma = 0.1\Omega$.

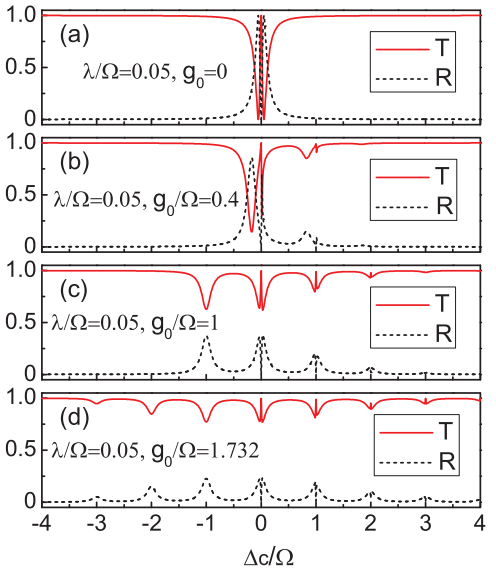

FIG. 5. (Color online) Single-photon transmission (reflection) spectra of the atom-optomechanical system for $\lambda < \Gamma$. The parameters are $\lambda = 0.05\Omega$, $\Delta_{ac} = 0$, $\gamma_a = 0$, and $\Gamma = 0.1\Omega$.

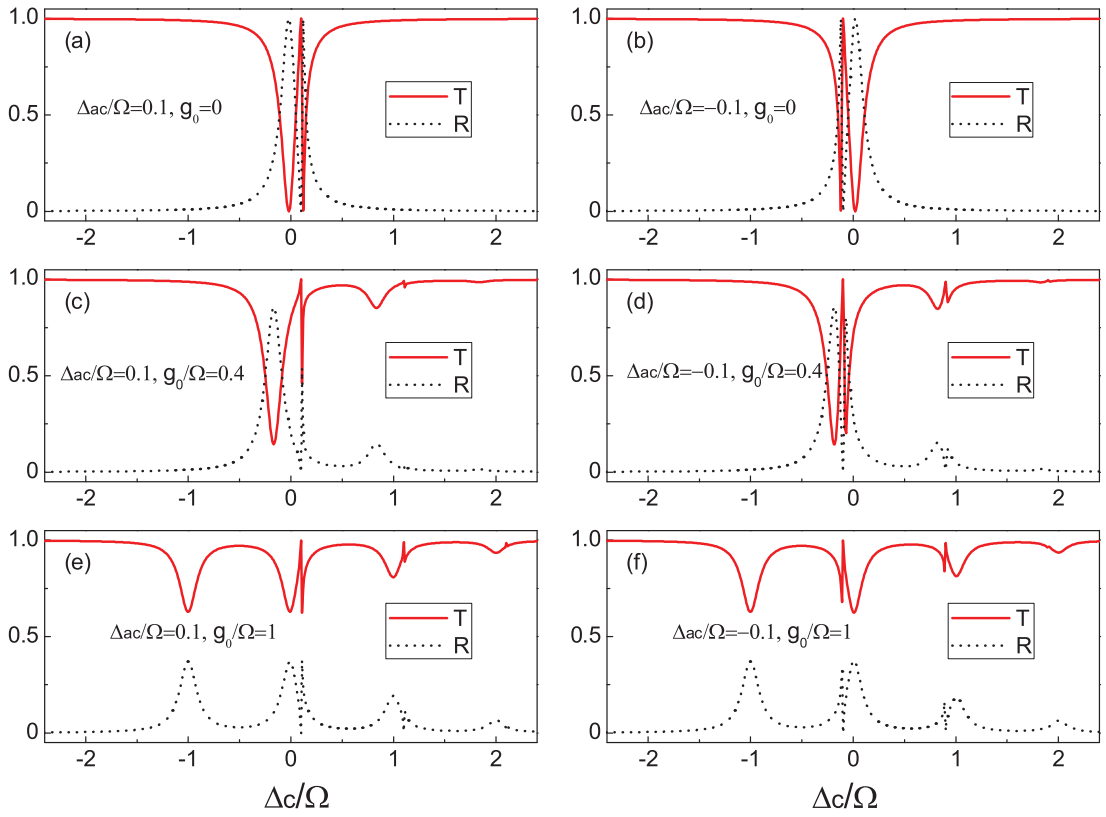

FIG. 6. (Color online) Single-photon transmission (reflection) spectra for detuned atom-cavity cases. In (a), (c), and (e), the atom-cavity detuning is $\Delta_{ac} = -0.1\Omega$; in (b), (d), and (f), $\Delta_{ac} = 0.1\Omega$. The other parameters are $\lambda = 0.05\Omega$, $\gamma_a = 0$, and $\Gamma = 0.1\Omega$.

$\Delta_c = -l\Omega$ ($l = 1, \ldots, m$), correspond to the $|0\rangle_c|g\rangle_a|0\rangle_b \rightarrow |\psi^{(-)}_{m-l}\rangle$ ($l = 1, \ldots, m$) transition, as shown in Figs. 5(c) and 5(d).

B. Single-photon transmission (reflection) coefficient: Effects of atom-cavity detunings and dissipations

We next consider the case of atom cavity to be detuned. When the optomechanical coupling strength $g_0 = 0$, for a photon on resonance with the atom $\Delta_c = \Delta_{ac}$, the transmission amplitude is always 1, as seen from Figs. 6(a) and 6(b), which was indicated in Ref. [2]. When entering the regime $g_0 \sim \Omega$, we can see that these maxima will appear at $\Delta_c = \Delta_{ac} + n\Omega$, corresponding to the $|0\rangle_c|g\rangle_a|0\rangle_b \rightarrow |0\rangle_c|e\rangle_a|n\rangle_b$ transitions, as shown in Figs. 6(c)–6(f).

We have mentioned in Sec. II that in our case the main dissipative processes originate from the decay of the atom. Figure 7 gives the transmission (reflection) spectrum of the dissipative atom case. If there are no dissipative processes, the sum of the transmission and reflection coefficients should satisfy $T + R = 1$. However, when the atom decay is included, the leakage of photons into nonwaveguided degrees of freedom can lead to $T + R < 1$, as shown in the gray thin lines in Fig. 7. Specifically, in the EIT-like cases with relatively small atom-cavity coupling strength ($\lambda \sim \Gamma$), the atom dissipation has a stronger effect on the transmission of a photon with detuning around $\Delta_c = n\Omega$ ($n = 0, 1, 2, \cdots$), as shown in Figs. 7(a), 7(c), and 7(e). On the contrary, in the Rabi-splitting like cases with strong atom-cavity coupling ($\lambda \gg \Omega \gg \Gamma$), the atom dissipation has a stronger effect on the transmission of a photon at the frequencies of resonant absorption, as shown in Figs. 7(b), 7(d), and 7(f).

C. The final reservoir occupation spectrum

We have discussed the transmission (reflection) coefficients of a monochromatic incident photon. Note that for an optomechanical system in a single-photon strong-coupling regime, the inelastic scattering should have an influential effect, resulting in a re-emitted photon with red-blue sideband frequency. This differs from the case of photon transmitting (reflecting) from a empty cavity, where the frequency of the photon remains unchanged after scattering. To see this point more clearly, we calculate the final reservoir occupation spectrum [23,28,29], which describes probability density for finding the single photon with a specific frequency of the transmission (reflection) fields. Let us consider an incident photon with a Gaussian-type spectral amplitude $\alpha(\Delta_c) = (2/\pi d^2)^{1/4} \exp[-(\Delta_c - \Delta_0)^2/d^2]$, where Δ_0 and d is the detuning and spectrum width of the photon, respectively. The according spectral density can be represented as $G = |\alpha|^2$. We plot in Fig. 8 the spectra $S_T(\Delta_c)$ and $S_R(\Delta_c)$ of resonantly incident single-photon (i.e., $\Delta_0 = 0$) scattering when the mirror is initially prepared in the ground state $|0\rangle_b$, with strong optomechanical coupling strength $g_0 = \Omega$ and different atom-cavity coupling strength λ. It can be seen from Fig. 8 that phonon sidebands appear in the spectrum in the

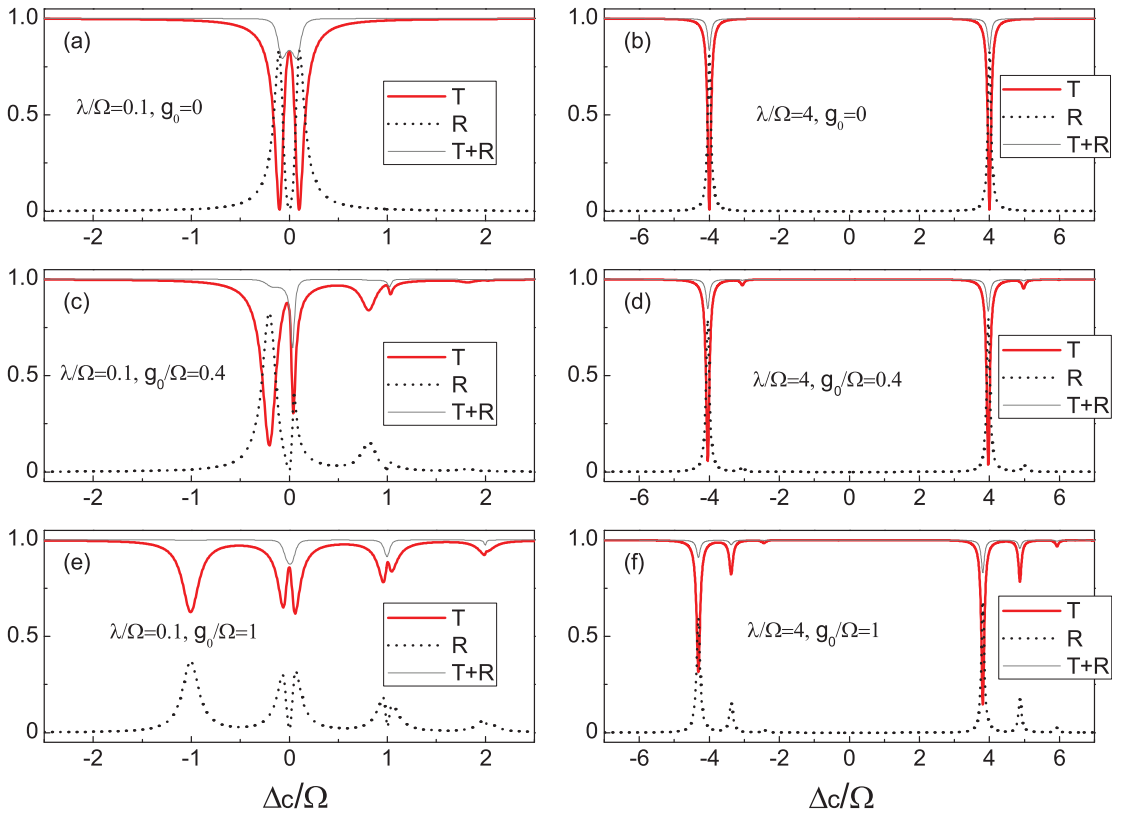

FIG. 7. (Color online) Single-photon transmission (reflection) spectra for dissipative atom cases ($\gamma_a = 0.01\Omega$). In (a), (c), and (e), the atom-cavity coupling strength is $\lambda = 0.1\Omega$; in (b), (d), and (f), $\lambda = 4\Omega$. The other parameters are $\Delta_{ac} = 0$ and $\Gamma = 0.1\Omega$.

strong-coupling regime with $g_0 \sim \Omega$. The dips in the spectrum $S_T(\Delta_c)$ correspond to the resonant transition from $|0\rangle_c|0\rangle_a|0\rangle_b$ to the excited states. Thus, after scattering, the probability density for finding the single photon at these frequencies decreases. And the peaks in the red sideband indicate that the re-emitted photon can lose its energy by $n\Omega$, leading to the final state $|0\rangle_c|0\rangle_a|n\rangle_b$ of system and increasing the value of $S_T(\Delta_c)$ at these transition frequencies.

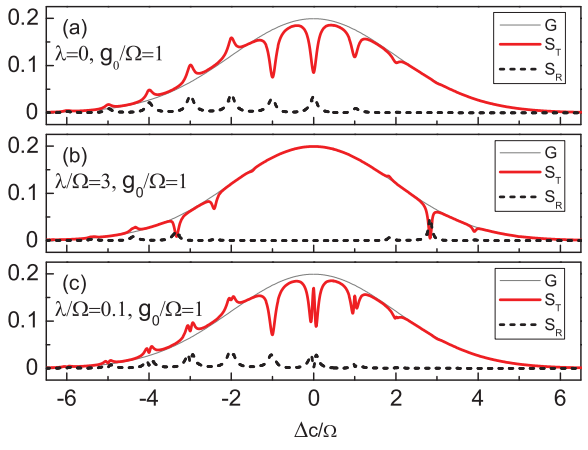

FIG. 8. (Color online) Transmitted (reflected) photon spectra $S_T(\Delta_c)$ ($S_R(\Delta_c)$). The parameters are $\Delta_0 = 0$, $d = 4\Omega$, $\Delta_{ac} = 0$, $\gamma_a = 0{,}01\Omega$, and $\Gamma = 0.1\Omega$. The gray thin curve is the spectral density G of incident photons.

IV. CONCLUSIONS

In summary, we have explored the single-photon transport in a single-mode waveguide coupled to a hybrid atom-optomechanical system in the single-photon strong-coupling regime, where multiple phonons are involved in the scattering. These spectra can characterize the mirror-cavity and atom-cavity couplings. An optomechanical coupling-dependent frequency shift and more sidebands appear in the transmission (reflection) spectra when the optical coupling strength increases. For the existence of atomic degrees of freedom, we can get a Rabi-splitting-like or an EIT-like spectrum, depending on the atom-cavity coupling strength.

In our calculation, we have assumed a zero temperature mechanical bath (i.e., the mean thermal excitation number $n_{\rm th} = 0$) and further ignored the mechanical decoherence processes for $\Gamma \gg \gamma_M$. If the influence of thermal noise is included, the mechanical oscillator initially prepared in its ground state will obtain some excited-state populations through the environment thermal heating. Thus the transmitted photon can absorb the energy of the phonons, resulting in additional sidebands in the transmitted photon spectrum. In addition, the thermal decoherence will lead to dephasing between the incident and re-emitted field [29].

Finally, we wish to make some further remarks on the possible experimental realizations of hybrid atom-optomechanical systems. Such a hybrid system can be possibly realized by directly combining the well-developed technology of optomechanical cavities with moving mirror [11–13] and trapping a single atom in cavity QED [35]. Also, this setup

may be more easily achieved using an on-chip circuit cavity electromechanics with a spiral inductor shunted by a parallel-plate capacitor, an analog of optomechanical cavity in a microwave domain [17], which can be easily coupled to a superconducting artificial atom using currently availabe circuit QED technology [7]. These systems may provide a quantum interference that allows the coherent transfer of quantum states between the mechanical oscillator and atoms, opening a door for coherent preparation and manipulation of micromechanical resonators [33].

ACKNOWLEDGMENTS

We thank Y. Li and S. Du for helpful discussions. This work was supported by the GRF (HKU7058/11P) and the CRF (HKU8/11G) of Hong Kong and the URC fund of HKU.

[1] J. T. Shen and S. Fan, Phys. Rev. Lett. **95**, 213001 (2005).
[2] J. T. Shen and S. Fan, Phys. Rev. A **79**, 023837 (2009).
[3] L. Zhou, Z. R. Gong, Y. X. Liu, C. P. Sun, and F. Nori, Phys. Rev. Lett. **101**, 100501 (2008).
[4] J. Claudon, J. Bleuse, N. S. Malik, M. Bazin, P. Jaffrennou, N. Gregersen, C. Sauvan, P. Lalanne, and Jean-Michel Gérard, Nat. Photon. **4**, 174 (2010).
[5] D. E. Chang, A. S. Sørensen, E. A. Demler, and M. D. Lukin, Nat. Phys. **3**, 807 (2007).
[6] O. Astafiev, A. M. Zagoskin, A. A. Abdumalikov Jr., Y. A. Pashkin, T. Yamamoto, K. Inomata, Y. Nakamura, and J. S. Tsai, Science **327**, 840 (2010).
[7] A. Wallraff, D. I. Schuster, A. Blais, L. Frunzio, R. S. Huang, J. Majer, S. Kumar, S. M. Girvin, and R. J. Schoelkopf, Nature (London) **431**, 162 (2004).
[8] T. Aoki, B. Dayan, E. Wilcut, W. P. Bowen, A. S. Parkins, T. J. Kippenberg, K. J. Vahala, and H. J. Kimble, Nature (London) **443**, 671 (2006).
[9] K. Srinivasan and O. Painter, Nature (London) **450**, 862 (2007).
[10] B. Dayan, A. S. Parkins, T. Aoki, E. P. Ostby, K. J. Vahala, and H. J. Kimble, Science **319**, 1062 (2008).
[11] T. J. Kippenberg and K. J. Vahala, Science **321**, 1172 (2008).
[12] F. Marquardt and S. M. Girvin, Physics **2**, 40 (2009).
[13] M. Aspelmeyer, T. J. Kippenberg, and F. Marquardt, arXiv:1303.0733.
[14] K. W. Murch, K. L. Moore, S. Gupta, and D. M. Stamper-Kurn, Nat. Phys. **4**, 561 (2008).
[15] F. Brennecke, S. Ritter, T. Donner, and T. Esslinger, Science **322**, 235 (2008).
[16] D. W. C. Brooks, T. Botter, S. Schreppler, T. P. Purdy, N. Brahms, and D. M. Stamper-Kurn, Nature **488**, 476 (2012).
[17] J. D. Teufel, T. Donner, D. Li, J. W. Harlow, M. S. Allman, K. Cicak, A. J. Sirois, J. D. Whittaker, K. W. Lehnert, and R. W. Simmonds, Nature **475**, 359 (2011).
[18] J. Chan, T. P. M. Alegre, A. H. Safavi-Naeini, J. T. Hill, A. Krause, S. Groblacher, M. Aspelmeyer, and O. Painter, Nature **478**, 89 (2011).
[19] J. Chan, A. H. Safavi-Naeini, J. T. Hill, S. Meenehan, and O. Painter, Appl. Phys. Lett. **101**, 081115 (2012).
[20] E. Verhagen, S. Deleglise, S. Weis, A. Schliesser, and T. J. Kippenberg, Nature **482**, 63 (2012).
[21] P. Rabl, Phys. Rev. Lett. **107**, 063601 (2011).
[22] A. Nunnenkamp, K. Børkje, and S. M. Girvin, Phys. Rev. Lett. **107**, 063602 (2011).
[23] Jie-Qiao Liao and C. K. Law, Phys. Rev. A **87**, 043809 (2013).
[24] Xun-Wei Xu, Yuan-Jie Li, and Yu-xi Liu, Phys. Rev. A **87**, 025803 (2013).
[25] A. Nunnenkamp, K. Børkje, and S. M. Girvin, Phys. Rev. A **85**, 051803 (2012).
[26] A. Kronwald and F. Marquardt, Phys. Rev. Lett. **111**, 133601 (2013).
[27] J. Qian, A. A. Clerk, K. Hammerer, and F. Marquardt, Phys. Rev. Lett. **109**, 253601 (2012).
[28] J. Q. Liao, H. K. Cheung, and C. K. Law, Phys. Rev. A **85**, 025803 (2012).
[29] Xue-Xin Ren, Hao-Kun Li, Meng-Yuan Yan, Yong-Chun Liu, Yun-Feng Xiao, and Qihuang Gong, Phys. Rev. A **87**, 033807 (2013).
[30] Marc-Antoine Lemonde, N. Didier, and A. A. Clerk, Phys. Rev. Lett. **111**, 053602 (2013).
[31] K. Børkje, A. Nunnenkamp, J. D. Teufel, and S. M. Girvin, Phys. Rev. Lett. **111**, 053603 (2013).
[32] Yong-Chun Liu, Yun-Feng Xiao, You-Ling Chen, Xiao-Chong Yu, and Qihuang Gong, Phys. Rev. Lett. **111**, 083601 (2013).
[33] K. Hammerer, M. Wallquist, C. Genes, M. Ludwig, F. Marquardt, P. Treutlein, P. Zoller, J. Ye, and H. J. Kimble, Phys. Rev. Lett. **103**, 063005 (2009); M. Wallquist, K. Hammerer, P. Zoller, C. Genes, M. Ludwig, F. Marquardt, P. Treutlein, J. Ye, and H. J. Kimble, Phys. Rev. A **81**, 023816 (2010).
[34] Daniel Breyer and Marc Bienert, Phys. Rev. A **86**, 053819 (2012).
[35] R. Miller, T. E. Northup, K. M. Birnbaum, A. Boca, A. D. Boozer, and H. J. Kimble, J. Phys. B **38**, S551 (2005).
[36] S.-L. Zhu, Z. D. Wang, and K. Yang, Phys. Rev. A **68**, 034303 (2003).
[37] Huaixiu Zheng, D. J. Gauthier, and H. U. Baranger, Phys. Rev. Lett. **107**, 223601 (2011).
[38] A. Blais, R. S. Huang, A. Wallraff, S. M. Girvin, and R. J. Schoelkopf, Phys. Rev. A **69**, 062320 (2004).
[39] S. E. Harris, Phys. Today **50**, 36 (1997).
[40] P. Rice and R. Brecha, Opt. Commun. **126**, 230 (1996).